Journal of Advanced Research in Numerical Heat Transfer

Journal homepage:
https://semarakilmu.com.my/journals/index.php/arnht/index
ISSN: 2735-0142

Forced Convection Flow of Nanofluid Within a Partially Filled Porous Straight Channel

Bashar Mahmood Ali[1,*]

[1] Department of Construction Engineering and Project Management, College of Engineering, Alnoor University, 41012, Mosul, Nineveh, Iraq

ARTICLE INFO

Article history:
Received 10 August 2024
Received in revised form 13 September 2024
Accepted 15 October 2024
Available online 30 November 2024

Keywords:
Heat transfer; Finite element method; Nusselt number; Darcy number

ABSTRACT

The present study examines the impact of nanoparticle flow and migration on heat transfer within a linear channel containing a partially porous medium. The study utilizes an Al_2O_3-water nanofluid to explore forced convective heat transfer, a topic that remains underexplored in existing literature, particularly in the context of porous channels. The porous channel is modeled using the Finite Element Method (FEM) for a steady flow, assuming thermal equilibrium between the solid phases and the nanofluid. A non-uniform distribution of nanoparticles within the channel is assumed, leading to the interdependence between the volume fraction distribution equation and the governing equations. A thorough analysis has been conducted on the impact of various parameters, including the Darcy number and Reynolds number. The findings indicate a direct relationship between the Reynolds number and the Nusselt number, with increases in the Reynolds number resulting in higher Nusselt numbers. Additionally, an increase in the Darcy number leads to an increase in the Nusselt number.

1. Introduction

Forced convection, a distinct heat transfer mode, relies on imposed fluid motion to enhance heat transfer rates, achieved through mechanisms such as ceiling fans, pumps, suction devices, or similar means. Widely employed by engineers for its high efficiency in transporting substantial thermal energy, convection is utilized in heating and air conditioning systems, electronics cooling, and various other technological domains [1-5]. Nanofluids have been investigated for their potential to manipulate or engineer thermophysical characteristics of conventional fluids by incorporating different types and concentrations of nanoparticles [6-9]. This offers a promising approach to improving overall system performance. The authors of the study utilized a two-dimensional (2D) lattice Boltzmann method (LBM) to conduct a numerical simulation of forced convection in a channel with an extended surface, involving three distinct nanofluids [10]. Results indicated that increasing Reynolds number values resulted in more significant heat transfer enhancement due to nanofluid presence.

* *Corresponding author.*
E-mail address: bashar.m@alnoor.edu.iq (Bashar Mahmood Ali)

https://doi.org/10.37934/arnht.27.1.6684

Extensive research has been conducted by the scientific community to explore techniques and strategies for enhancing heat transfer rates in thermal devices, predominantly focusing on surface modification or nanofluid utilization while considering both active and passive methodologies [11,12]. Porous media has applications in various applied science branches, such as cooling miniature electronic components, storing nuclear waste, radioactive materials, and oil recovery. Partially filled porous channels had garnered attention as potential solutions due to their pore-solid structural orientation. According to Bhowmick *et al.,* [13], heat transfer rates increased rapidly while experiencing only a slightly higher pressure drop. A study using numerical methods investigated forced convection within a channel featuring both an open cavity and a porous medium [14]. The opposing forced flow configuration exhibited superior thermal efficiency concerning the maximum temperature of the nanofluid and the average Nusselt number. The authors analyzed the impact of forced convection on a two-dimensional microchannel, examining a porous medium containing water/FMWCNT nanofluid [15]. A computational investigation of forced convection effects of Al_2O_3-CuO-water nanofluid in a partitioned cylinder within a porous medium, focusing on magnetohydrodynamics, was documented by Aminian *et al.,* [16], demonstrating the influence of both the porous medium and nanoparticles on heat transfer results.

In various applications, such as solar collectors, absorbers may have different geometries, like wavy or corrugated, although they are commonly manufactured as shallow enclosures with flat surfaces. Using undulated or fluted conduits was one method to augment thermal exchange effectiveness in industrial conveyance mechanisms [17,18]. A lattice Boltzmann technique was used to investigate the uniform vertical magnetic field's impact on the thermo-hydrodynamics of a nanofluid using a slightly porous channel, as reported by Ashorynejad and Zarghami [19], examining thermo-hydrodynamics of flow and active factors' effects, including the solid volume fraction of nanoparticles, pressure gradient, magnetic field, and porous layer permeability. Armaghani *et al.,* [1] investigated the effects of nanoparticle flow and migration on heat transfer in a straight channel that is filled with a porous medium. The research examined forced convective heat transfer in a porous channel for nanofluids, utilizing a local thermal non-equilibrium model that considers the pure fluid, solid, and nanoparticle phases. A thorough examination was carried out to determine the impact of the Lewis number, Schmidt number, and modified diffusivity ratio (Nbt) on the process of heat transfer. The results suggest that an augmentation in the Lewis number resulted in a reduction in the non-dimensional heat flux assimilated by the fluid.

Recent advancements in the study of forced convection in nanofluids within porous media have contributed significantly to understanding heat transfer mechanisms. Researchers have increasingly focused on improving the thermophysical properties of nanofluids by introducing novel nanoparticle types and varying concentrations [20-22]. For instance, Younes *et al.,* [6] explored the thermal conductivity enhancement of various nanofluids, emphasizing the role of nanoparticle size and volume fraction in improving heat transfer rates in porous systems. Some research has shown the promising heat transfer characteristics of engine oil embedded with nanoparticles such as SWCNTs, MWCNTs, and TiO_2, in porous stretching cylinders [23,24]. This combination offers potential applications in improving the efficiency of thermal systems due to enhanced thermal conductivity and fluid stability in high-temperature environments [25,26]. Similarly, the computational analysis of gyrotactic microbes combined with variable viscosity effects has been instrumental in uncovering the dynamic interactions within chemically reactive nanofluid systems [27]. Such studies provide valuable insights into complex flow dynamics relevant to industrial applications requiring precise thermal regulation and nanofluid stability. Additionally, Ahmed *et al.,* [11] investigated the application of MXene-based nanofluids in porous media, demonstrating their superior heat transfer capabilities in cooling systems and energy storage applications.

In recent years, attention has also shifted towards the influence of motile microorganisms and chemical reactions in viscoelastic fluid flows [28]. Specifically, the combination of thermal radiation with exponentially stretching sheets in Darcy-Forchheimer porous mediums has demonstrated enhanced heat transfer efficiencies [28,29]. Furthermore, magnetohydrodynamic (MHD) studies have investigated the characteristics of MWCNT, SWCNT, Cu, and water-based nanofluids in magnetized flows, showing how Soret and Dufour effects influence thermal performance in the power-law-driven systems [30,31]. These findings are critical for applications in cooling technologies and energy systems where precise control of thermal parameters is required.

Despite these advancements, certain gaps remain. While several studies have examined the forced convection of nanofluids, a comprehensive analysis of the interaction between nanoparticle migration and flow characteristics in partially porous media is still lacking. Armaghani *et al.,* [1] and Nazari *et al.,* [2] have highlighted the influence of nanoparticle migration on heat transfer rates, but their studies primarily focus on fully porous or homogeneously porous systems, leaving partially porous configurations underexplored. Moreover, existing studies often concentrate on traditional nanofluids such as Al_2O_3-water and TiO_2-water, with the limited investigation into hybrid nanofluids or novel nanoparticle compositions [32,33]. This presents an opportunity for further research to assess how hybrid or newer nanofluids perform under forced convection in porous channels. The current study aims to fill these gaps by examining forced convection in a partially porous medium using an Al_2O_3-water nanofluid. This approach will provide new insights into the impact of nanoparticle migration and porous channel configuration on heat transfer performance, addressing the limitations noted in previous studies.

The Lattice Boltzmann Method was employed to investigate the impact of a uniform vertical magnetic field on the flow behavior and heat transfer associated with fluid-solid coupling in a channel that was partially filled with a porous medium. The nanofluid used in Javaherdeh and Ashorynejad [34] study was composed of Al_2O_3-water and exhibited temperature-sensitive properties. The study presented a novel correlation for the density of Al_2O_3-water nanofluid, which was found to be dependent on temperature. Additionally, the reliability of the step approximation for porous medium boundaries was demonstrated. The study examined the impact of varying nanoparticle volume fractions and magnetic field strengths on heat transfer rates. The study's findings suggest that an increase in the volume fraction of nanoparticles led to a corresponding increase in the average temperature, velocity, and Nusselt number. An experiment by Baragh *et al.,* [35] was conducted on a single-phase flow of air in a channel with a circular cross-section and varying configurations of porous media. The study examined alterations in hydrodynamic parameters, enhancements in heat transfer facilitated by porous media within a channel, and the pressure drop that arises from the use of porous media. The experimental findings indicate that the existence of porous media facilitated the transfer of thermal flux from the channel walls to the fluid. This was attributed to the uniform interstitial space and high conductivity of the porous media. Moreover, the average temperature of the fluid escalated, resulting in a reduction of the temperature gradient between the channel wall and the mean temperature of the fluid.

The present study offers significant contributions to the field of heat transfer in nanofluids, particularly within partially porous channels, by addressing gaps left in previous works. While numerous studies have explored forced convection in fully porous or homogeneously porous systems, the interaction between nanoparticle migration and flow characteristics in partially filled porous media has been largely overlooked. Furthermore, most existing research has concentrated on traditional nanofluids such as Al_2O_3-water and TiO_2-water, with limited attention given to the unique behaviors of novel and hybrid nanofluids. By focusing on the Al_2O_3-water nanofluid in a partially porous channel, this study provides new insights into the effect of porous configurations on heat transfer performance. Additionally, the use of the Finite Element Method (FEM) to simulate the flow and thermal behavior introduces a more detailed analysis of the interactions between the Darcy number, Reynolds number, and Nusselt number. These contributions not only enhance the understanding of nanofluid dynamics in porous media but also offer practical implications for the design and optimization of thermal systems in industries such as energy storage, cooling technologies, and electronic thermal management.

2. Mathematical Formulation

The forced convection flow into a two-dimensional horizontal channel has length d and height h is described in Figure 1. The dimensions of the model used in this study are as follows: The channel has a length of 10 cm and a height of 1 cm. The thickness of the porous region is 0.5 cm. The Al_2O_3 nanoparticles utilized in the nanofluid have a diameter of 20 nm. These dimensions are critical to the accurate formulation and analysis of the forced convection flow within the partially porous channel. An isothermal heater remains at the bottom surface of the channel. The inlet fluid flow including cold temperature (T_c) includes approaching the channel of the left section with consistent horizontal velocity left vertical surface. In contrast, the fluid outlet field remains flowing in the right adiabatic section of the channel among fixed pressure (p=0). The space between the channel surfaces is filled with water-Al_2O_3 nanoparticles (nanofluid).

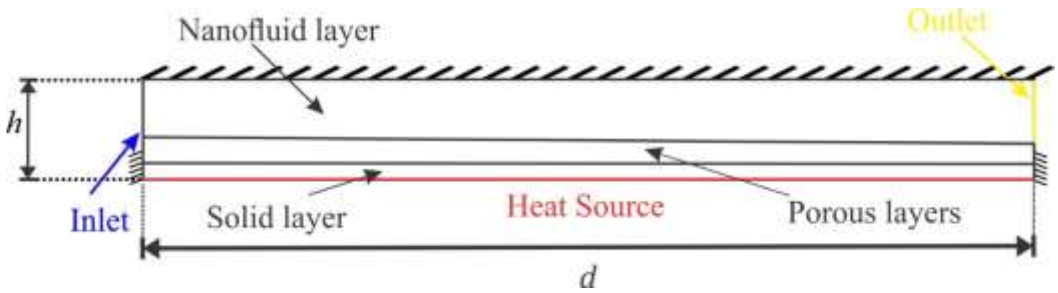

Fig. 1. The model geometry of the problem with the coordinate system [36].

The associated equations of the laminar flow and temperature distribution with the assumptions specified are addressed as follows:

For the nanofluid layer:

$$\frac{\partial u}{\partial x}+\frac{\partial v}{\partial y}=0, \tag{1}$$

$$u\frac{\partial u}{\partial x}+v\frac{\partial u}{\partial y}=-\frac{1}{\rho_{nf}}\frac{\partial p}{\partial x}+\nu_{nf}\left(\frac{\partial^2 u}{\partial x^2}+\frac{\partial^2 u}{\partial y^2}\right), \tag{2}$$

$$u\frac{\partial v}{\partial x}+v\frac{\partial v}{\partial y}=-\frac{1}{\rho_{nf}}\frac{\partial p}{\partial y}+\nu_{nf}\left(\frac{\partial^2 v}{\partial x^2}+\frac{\partial^2 v}{\partial y^2}\right), \tag{3}$$

$$\frac{\partial T}{\partial x}+v\frac{\partial T}{\partial y}=\alpha_{nf}\left(\frac{\partial^2 T}{\partial x^2}+\frac{\partial^2 T}{\partial y^2}\right). \tag{4}$$

For the porous layer:

$$\frac{\partial u_m}{\partial x}+\frac{\partial v_m}{\partial y}=0, \tag{5}$$

$$\frac{\rho_{nf}}{\varepsilon^2}\left(u_m\frac{\partial u_m}{\partial x}+v_m\frac{\partial u_m}{\partial y}\right)=-\frac{\partial p}{\partial x}+\frac{\mu_{nf}}{\varepsilon}\left(\frac{\partial^2 u_m}{\partial x^2}+\frac{\partial^2 u_m}{\partial y^2}\right)\left(\frac{\mu_{nf}}{K}u_m-\frac{1.75}{\sqrt{150}\varepsilon^{3/2}}\frac{\rho_{nf}u_m|\mathbf{u}|}{\sqrt{K}}\right), \tag{6}$$

$$\frac{\rho_{nf}}{\varepsilon^2}\left(u_m\frac{\partial v_m}{\partial x}+v_m\frac{\partial v_m}{\partial y}\right)=-\frac{\partial p}{\partial y}+\frac{\mu_{nf}}{\varepsilon}\left(\frac{\partial^2 v_m}{\partial x^2}+\frac{\partial^2 v_m}{\partial y^2}\right)-\left(\frac{\mu_{nf}}{K}v_m-\frac{1.75}{\sqrt{150}\varepsilon^{3/2}}\frac{\rho_{nf}v_m|\mathbf{u}|}{\sqrt{K}}\right), \tag{7}$$

$$u_m\frac{\partial T_m}{\partial x}+v_m\frac{\partial T_m}{\partial y}=\frac{\varepsilon k_{nf}}{(\rho C_p)_{nf}}\left(\frac{\partial^2 T_m}{\partial x^2}+\frac{\partial^2 T_m}{\partial y^2}\right). \tag{8}$$

The subscripts nf, m, s and w view the nanofluid layer, porous layer (nanofluid phase), porous layer (solid phase), and solid surface, respectively. x and y are the fluid velocity elements, and K is the permeability of the porous medium which is determined as [37]:

$$K=\frac{\varepsilon^3 d_m^2}{150(1-\varepsilon)^2}. \tag{9}$$

Here d_m represents the average particle size of the porous bed. We specified the employed thermo-physical properties of the nanofluid as follows:

$$\begin{aligned}
&(\rho C_p)_{nf}=(1-\phi)(\rho C_p)_f+\phi(\rho C_p)_p,\\
&\alpha_{nf}=\frac{k_{nf}}{(\rho C_p)_{nf}},\\
&\rho_{nf}=(1-\phi)\rho_f+\phi\rho_p,\\
&(\rho\beta)_{nf}=(1-\phi)(\rho\beta)_f+\phi(\rho\beta)_p,\\
&\frac{k_{nf}}{k_f}=1+4.4\mathrm{Re}_B^{0.4}\mathrm{Pr}^{0.66}\left(\frac{T}{T_{fr}}\right)^{10}\left(\frac{k_p}{k_f}\right)^{0.03}\phi^{0.66},\\
&\frac{\mu_{nf}}{\mu_f}=1/\left(1-34.87\left(d_p/d_f\right)^{-0.3}\phi^{1.03}\right).
\end{aligned} \tag{10}$$

where Re_B is defined as:

$$\mathrm{Re}_B=\frac{\rho_f u_B d_p}{\mu_f},\quad u_B=\frac{2k_b T}{\pi\mu_f d_p^2}. \tag{11}$$

The molecular diameter of the used liquid (water) is given by:

$$d_f = \frac{6M}{N\pi\rho_f}. \tag{12}$$

We show the non-dimensional variables that were used:

$$(X,Y) = \frac{(x,y)}{L},\ U_{nf,m} = \frac{u_{nf,m}L}{\alpha_f},\ V_{nf,m} = \frac{v_{nf,m}L}{\alpha_f},\ \theta_{nf} = \frac{T_{nf}-T_c}{T_h-T_c},$$
$$\theta_m = \frac{T_m-T_c}{T_h-T_c},\ P = \frac{pL^2}{\rho_f\alpha_f^2},\ k_{eff} = \varepsilon k_{nf} + (1-\varepsilon)k_m,\ C_F = \frac{1.75}{\sqrt{150}}. \tag{13}$$

As a result, the dimensionless governing equations are as follows:
In the nanofluid layer:

$$\frac{\partial U}{\partial X} + \frac{\partial V}{\partial Y} = 0, \tag{14}$$

$$U\frac{\partial U}{\partial X} + V\frac{\partial U}{\partial Y} = -\frac{\partial P}{\partial X} + \frac{1}{Re}\frac{\rho_f}{\rho_{nf}}\frac{\mu_{nf}}{\mu_f}\left(\frac{\partial^2 U}{\partial x^2} + \frac{\partial^2 U}{\partial Y^2}\right), \tag{15}$$

$$U\frac{\partial V}{\partial X} + V\frac{\partial V}{\partial Y} = -\frac{\partial P}{\partial Y} + \frac{1}{Re}\frac{\rho_f}{\rho_{nf}}\frac{\mu_{nf}}{\mu_f}\left(\frac{\partial^2 V}{\partial X^2} + \frac{\partial^2 V}{\partial Y^2}\right), \tag{16}$$

$$U\frac{\partial \theta}{\partial X} + V\frac{\partial \theta}{\partial Y} = \frac{\alpha_{nf}}{\alpha_f}\frac{1}{\Pr Re}\left(\frac{\partial^2 \theta}{\partial X^2} + \frac{\partial^2 \theta}{\partial Y^2}\right), \tag{17}$$

$$\frac{\partial^2 \theta_s}{\partial x^2} + \frac{\partial^2 \theta_s}{\partial y^2} = 0,$$

In the porous layer:

$$\frac{\partial U_m}{\partial X} + \frac{\partial V_m}{\partial Y} = 0, \tag{18}$$

$$\frac{1}{\varepsilon^2}\left(U_m\frac{\partial U_m}{\partial X} + V_m\frac{\partial U_m}{\partial Y}\right) = -\frac{\partial P}{\partial X} + \frac{\rho_f}{\rho_{nf}}\frac{\mu_{nf}}{\mu_f}\frac{\Pr}{\varepsilon}\left(\frac{\partial^2 U_m}{\partial X^2} + \frac{\partial^2 U_m}{\partial Y^2}\right) - \frac{\rho_f}{\rho_{nf}}\frac{\mu_{nf}}{\mu_f}\frac{\Pr}{Da}U_m - \frac{C_F\sqrt{U_m^2+V_m^2}}{\sqrt{Da}}\frac{U_m}{\varepsilon^{3/2}}, \tag{19}$$

$$\frac{1}{\varepsilon^2}\left(U_m\frac{\partial V_m}{\partial X}+V_m\frac{\partial V_m}{\partial Y}\right)=-\frac{\partial P}{\partial Y}+\frac{\rho_f}{\rho_{nf}}\frac{\mu_{nf}}{\mu_f}\frac{\Pr}{\varepsilon}\left(\frac{\partial^2 V_m}{\partial X^2}+\frac{\partial^2 V_m}{\partial Y^2}\right)-\frac{\rho_f}{\rho_{nf}}\frac{\mu_{nf}}{\mu_f}\frac{\Pr}{Da}V_m -\frac{C_F\sqrt{U_m^2+V_m^2}}{\sqrt{Da}}\frac{V_m}{\varepsilon^{3/2}}, \tag{20}$$

$$\frac{1}{\varepsilon}\left(U_m\frac{\partial \theta_m}{\partial X}+V_m\frac{\partial \theta_m}{\partial Y}\right)=\frac{k_{eff}}{k_f}\frac{(\rho C_p)_f}{(\rho C_p)_{nf}}\left(\frac{\partial^2 \theta_m}{\partial X^2}+\frac{\partial^2 \theta_m}{\partial Y^2}\right). \tag{21}$$

The dimensionless boundary conditions of Eq. (18) and (21) are:

On the bottom heated wavy wall:
$U=V=0,\ \theta=1,\ A(1-\cos(2N\pi Y)),\ 0\le X\le 1,$
On the top cold horizontal wall:

$$U=\lambda+S\frac{\mu_{nf}}{\mu_f}\frac{\partial U}{\partial Y}, V=0,\ \theta=0,\ 0\le X\le 1,\ Y=1, \tag{22}$$

On the left and right adiabatic vertical walls:
$U=V=0,\ \frac{\partial \theta}{\partial X}=0,\ X=0,1,\ 0\le Y\le 1, \theta=\theta_s,$
at the solid surface, $U=V=0,\ \frac{\partial \theta}{\partial n}=K_r\frac{\partial \theta_s}{\partial n}$

Over the solid cylinder's surface, where the thermal conductivity ratio is. At the heated bottom wavy surface, the local Nusselt number is computed as follows:

$$Nu_{nf}=\frac{h\,L}{k_{nf}}=-\frac{k_{nf}}{k_f}\frac{\partial \theta}{\partial n}L, \qquad \frac{\partial \theta}{\partial n}=\frac{1}{L}\sqrt{\left(\frac{\partial \theta}{\partial X}\right)^2+\left(\frac{\partial \theta}{\partial Y}\right)^2} \tag{23}$$

The average Nusselt number may also be determined by integrating the local Nusselt number over the wavy bottom partition, which is described as follows:

$$\overline{Nu}_{nf}=\frac{1}{W}\int_0^W Nu\ \mathrm{d}W \tag{24}$$

The boundary conditions applied in this study are critical in simulating realistic physical scenarios commonly found in engineering applications such as heat exchangers and cooling systems. At the inlet of the channel, a uniform velocity profile with a cold temperature (T_c) is applied, which represents a situation where fluid enters the channel at a known velocity and temperature [38]. This is a common condition in controlled fluid flow systems where the fluid flow is fully developed far upstream. The outlet boundary condition involves a constant pressure with a zero-velocity gradient, indicating that the fluid exits the channel into an area with ambient pressure, such as a reservoir or the atmosphere. This condition ensures smooth flow out of the domain and avoids numerical instabilities in the simulation.

The walls of the channel are subject to specific thermal conditions. The bottom wall is heated isothermally, simulating a surface with a constant temperature, which is typical in many industrial applications where controlled heat flux is applied, such as in heat exchangers. Meanwhile, the top wall is assumed to be adiabatic, meaning that no heat transfer occurs across this boundary, which models an insulated surface that prevents energy loss [39]. This ensures that heat transfer is restricted to the interaction between the fluid and the porous medium inside the channel.

At the interface between the nanofluid and the porous medium, continuity conditions are applied to ensure that the temperature and velocity fields transition smoothly between the two regions. This is essential to accurately capture the heat transfer and flow behavior across the porous and non-porous regions, reflecting real-world systems where different materials or media are in contact. By defining these boundary conditions, the study aims to replicate realistic operational scenarios and provide insight into the heat transfer dynamics within a porous channel, which is relevant to a wide range of applications in thermal management and fluid dynamics.

3. Numerical Method and Validation

The governing dimensionless Eq. (18)-(12) are solved using the finite element method under the boundary constraints Eq. (22). The computing domain is divided into triangular sections. Triangular Lagrange finite elements of various orders are employed for each of the flow variables within the computational domain. To create the residuals for each conservation equation, the approximations are substituted into the governing equations. To simplify the nonlinear variables in the momentum equations, a Newton-Raphson iteration method was used. The solution is converged when the relative error for each variable meets the following convergence conditions.

The finite element method (FEM) was employed to solve the governing equations, and a mesh independence study was conducted to ensure that the results are not dependent on the mesh size. Mesh densities of 5,000, 10,000, 20,000, and 40,000 elements were tested, and the Nusselt number and velocity profiles were compared for each case. The results show that the Nusselt number stabilizes at 24.2 for a mesh density of 20,000 elements, with further refinement showing negligible change. This confirms that a mesh size of 20,000 elements is sufficient to achieve accurate results while maintaining computational efficiency. The convergence criteria for the numerical solution were based on the relative error between successive iterations. The solution was considered converged when the relative error for temperature and velocity variables dropped below 10^{-6}, ensuring both high accuracy and computational feasibility.

In this study, we assumed thermal equilibrium between the solid phases (nanoparticles) and the nanofluid. This means that the temperature of the nanoparticles is equal to that of the surrounding fluid at every point in the domain. This assumption is valid for systems where thermal diffusion is much faster than fluid flow. However, in cases involving high nanoparticle concentrations or large temperature gradients, this assumption might not hold, and non-equilibrium conditions could arise. Future studies may focus on exploring the effects of non-equilibrium conditions in such systems.

$$\left|\frac{\Gamma^{i+1}-\Gamma^{i}}{\Gamma^{i+1}}\right|\leq 10^{-6}, \tag{25}$$

To verify the results, the current results are compared to the experimental and numerical findings supplied by Kalteh *et al.,* [36] for the problem of forced convection heat transfer of nanofluid within a horizontal microchannel heat sink, as indicated in Figure 2. This comparison assumes that the current numerical code is accurate.

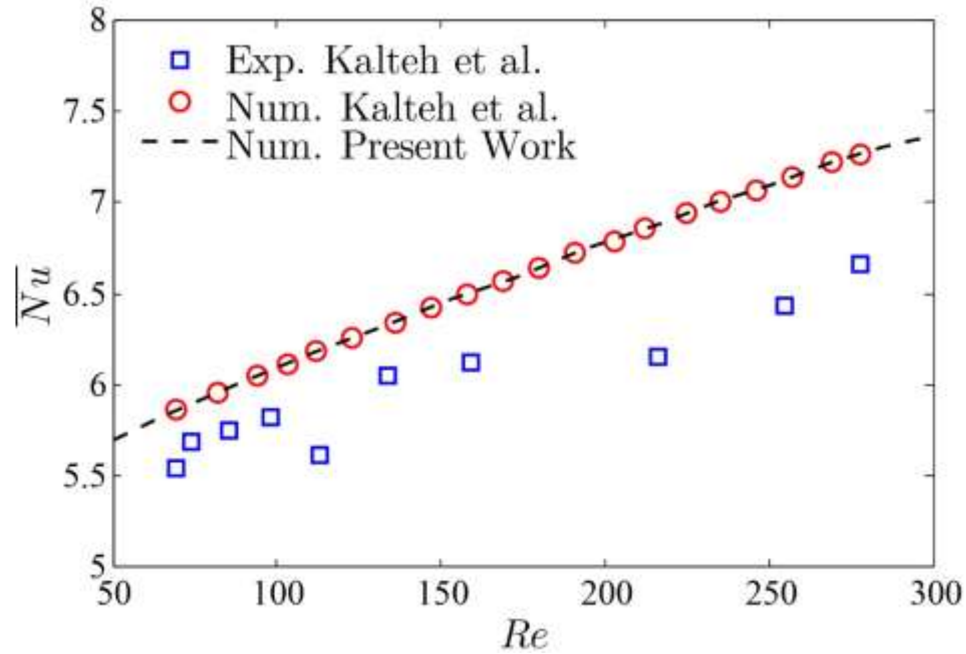

Fig. 2. The model geometry of the problem with the coordinate system

Figures 3 and 4 illustrate the temperature gradient during the flow of the liquid inside the proposed channel, and its dependence on both the particle size in the liquid and the level of permeability in the channel. Figure 3 shows the temperature gradient for different values of the Reynolds number, while Figure 4 demonstrates this dependence using various Darcy values.

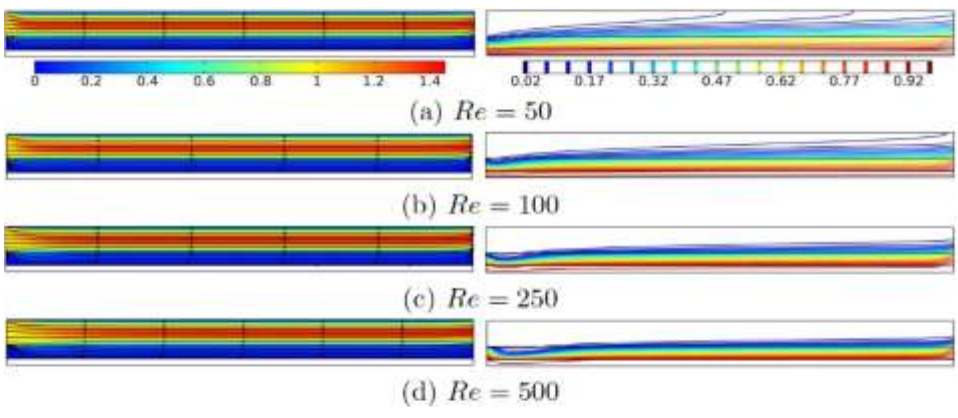

Fig. 3. Heat transfer is influenced by different values of the Reynold number (Re)

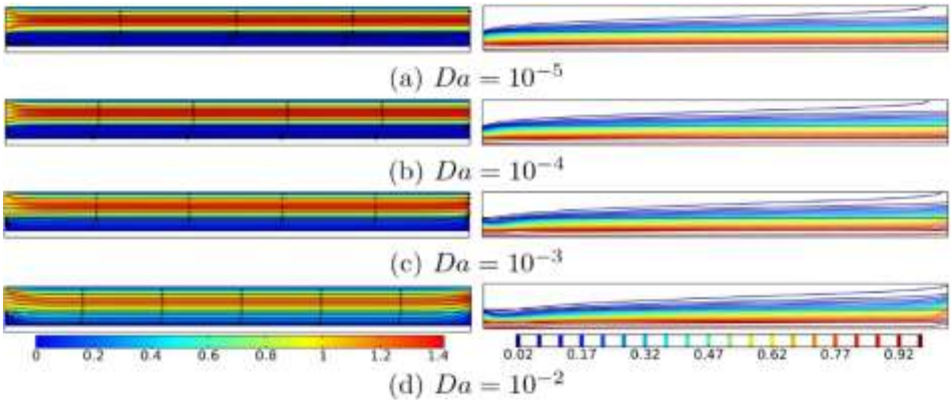

Fig. 4. Heat transfer is influenced by different values of the Darcy number (Da)

4. Mesh Verification

To ensure the accuracy of the numerical results and eliminate dependence on mesh size, a mesh independence study was conducted. The study involved running simulations with different mesh densities and comparing the resulting Nusselt number (Nu) and velocity profiles. The mesh sizes ranged from coarse to fine, with element counts of 5,000, 10,000, 20,000, and 40,000. The results, presented in Table 1, demonstrate that the Nusselt number increased slightly with mesh refinement. However, the difference in results between 20,000 and 40,000 elements was negligible, with the Nusselt number stabilizing at 24.2. This suggests that a mesh size of 20,000 elements is sufficient to achieve accurate results while maintaining computational efficiency. Therefore, this mesh density was used for all subsequent simulations.

Table 1
Mesh independence study results

Mesh Size (number of elements)	Nusselt Number	Change in Nu (%)
5 000	23.6	-
10 000	24.0	1.69
20 000	24.2	0.83
40 000	24.2	0.00

5. Results and Discussion

For all volume fractions (φ), Nu and Re have a clear positive correlation. As the Reynolds number increases, indicating a transition toward more turbulent flow, the Nusselt number also increases, suggesting enhanced convective heat transfer [40] (see Figure 5). This trend is consistent across all nanoparticle concentrations. The presence of nanoparticles significantly enhances the Nusselt number compared to the base fluid (φ=0). As the nanoparticle volume fraction increases from 0 to 0.04, there is a noticeable increase in the Nusselt number for a given Reynolds number. This indicates that the inclusion of nanoparticles improves heat transfer performance due to the higher thermal conductivity of the nanofluid. At a Reynolds number of 500, the Nusselt number ranges from approximately 18 for φ=0 to 24 for φ=0.04. This relative increase highlights the effectiveness of higher nanoparticle concentrations in enhancing heat transfer. Specifically, the enhancement is more pronounced at higher Reynolds numbers, suggesting that turbulent conditions amplify nanoparticle inclusion's benefits [41]. The incremental benefit of increasing φ diminishes slightly at higher concentrations. For instance, the difference in Nu between φ=0.03 and φ=0.04 is less pronounced than between φ=0.01 and φ=0.02. This suggests a potential asymptotic behavior where additional nanoparticles contribute marginally to heat transfer enhancement beyond a specific concentration. These findings have practical implications for the design of heat exchangers and cooling systems. By optimizing the nanoparticle concentration, engineers can significantly enhance heat transfer rates, improving system efficiency and performance [38, 42-44]. However, the diminishing returns at higher concentrations must be considered to avoid unnecessary costs and potential issues such as increased viscosity [45].

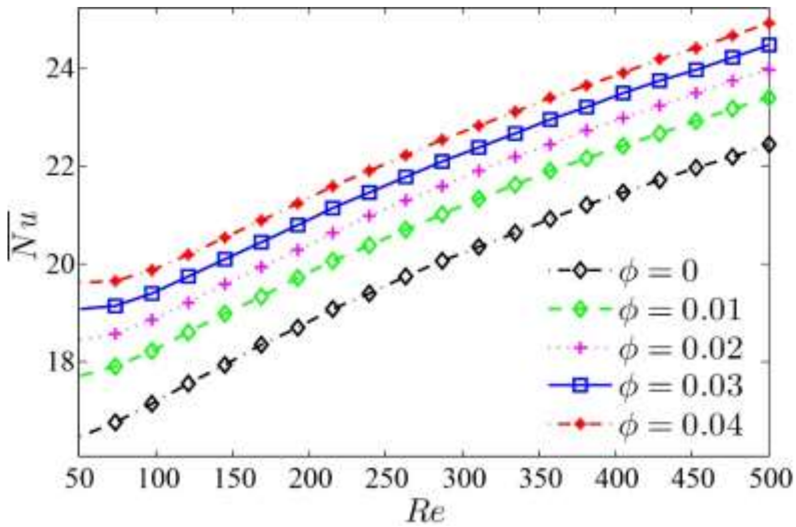

Fig. 5. The relation between Reynold Number (Re) and Nusselt number (Nu) based on particle sizes

As the particle size in the liquid increases, the Darcy number will change accordingly. As shown in Figure 6, when the Darcy value ranges from 10^{-6} to 10^{-4}, there is a constant value of the Nusselt number for each particle size. However, when the Darcy value starts to increase between 10^{-4} and 10^{-2}, a sharp increase in the Nusselt number value can be observed, while the difference in the Nusselt number between closely sized particles remains constant. As the Reynolds number increases, the Nusselt number also increases across all nanoparticle concentrations. This relationship suggests that higher flow velocities enhance convective heat transfer [46]. The inclusion of nanoparticles significantly improves the Nusselt number compared to the base fluid (φ=0). Each increment in nanoparticle concentration results in a higher Nusselt number, demonstrating the efficacy of nanoparticles in enhancing heat transfer due to their superior thermal properties [47]. At very low Reynolds numbers (ranging from 10^{-6} to 10^{-4}), the impact of nanoparticles on the Nusselt number is less pronounced. However, as the Reynolds number increases beyond 10^{-4}, the benefits of higher nanoparticle concentrations become more significant. This indicates that nanoparticle-induced enhancements are more effective at higher flow velocities [48].

The relationship between Nu and Re is non-linear, particularly evident at higher Reynolds numbers (above 10^{-3}). This non-linearity is more pronounced for higher nanoparticle concentrations. The curves exhibit an accelerating increase in the Nusselt number, suggesting a complex interaction between flow dynamics and heat transfer mechanisms in the presence of nanoparticles. These observations have important implications for the design and optimization of thermal systems. In applications requiring high heat transfer rates, incorporating nanoparticles into the working fluid can significantly enhance performance [49]. The non-linear relationship at higher Reynolds numbers indicates that optimal nanoparticle concentrations should be carefully selected based on the specific flow conditions to maximize heat transfer efficiency [50]. At very low Reynolds numbers, the heat transfer enhancement due to nanoparticles is relatively modest. This is likely due to the dominance of conductive heat transfer mechanisms over convective ones in this regime. However, even in this regime, the presence of nanoparticles provides a noticeable improvement over the base fluid. Higher nanoparticle concentrations and increased flow velocities lead to substantial improvements in the Nusselt number, making nanofluids a promising choice for enhancing thermal efficiency in various applications [51]. The non-linear behavior observed at higher Reynolds numbers suggests that the interplay between flow and thermal properties becomes increasingly complex, requiring detailed analysis for optimal system design.

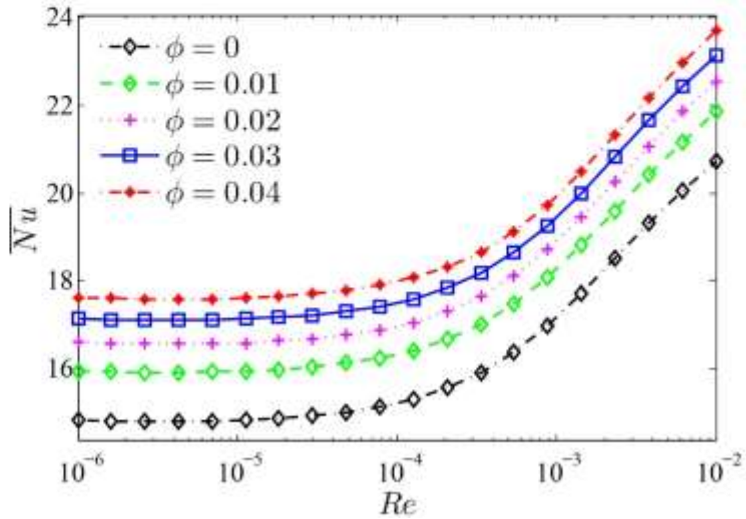

Fig. 6. The relation between Darcy Number (Da) and Nusselt number (Nu) based on particle sizes

Regarding the permeability in our study, the relationship between the Reynolds number and the Nusselt number is clearly illustrated in Figure 7. It is observed that increasing the permeability in the channel leads to an increase in the value of the Reynolds number, followed by an increase in the value of the Nusselt number. Furthermore, as the permeability value increases, the difference in the Nusselt number between previous values decreases. This is evident when the permeability value is between 0.06 and 0.08. the relationship between the Nusselt number (Nu) and the Reynolds number (Re) for different porosity values (ε) in a fluid flowing through a partially porous channel. The Nusselt number, representing the convective heat transfer coefficient, is plotted on the vertical axis, while the Reynolds number, indicating the flow regime, is plotted on the horizontal axis. The porosity values range from ε=0.2 to ε=0.8, with different line styles corresponding to each porosity level. Across all porosity values, there is a clear positive correlation between Nu and Re. As the Reynolds number increases, the Nusselt number also increases, suggesting enhanced convective heat transfer with higher flow velocities [52]. This trend is consistent across all porosity levels. Higher porosity values (ε=0.8) consistently result in higher Nusselt numbers compared to lower porosity values (ε=0.2). This indicates that a more porous medium enhances heat transfer efficiency, likely due to improved fluid mixing and higher surface area for heat exchange. At a Reynolds number of 500, the Nusselt number ranges from approximately 17 for ε=0.2 to around 24 for ε=0.8. This relative increase highlights the significant role of porosity in enhancing heat transfer. The enhancement becomes more pronounced at higher Reynolds numbers, indicating that the benefits of higher porosity are amplified under turbulent flow conditions [53].

The incremental benefit of increasing porosity diminishes slightly at higher porosity values. For instance, the difference in Nu between ε=0.6 and ε=0.8 is less pronounced than between ε=0.2and ε=0.4. This suggests a potential asymptotic behavior where beyond a certain porosity, additional increases yield diminishing returns in heat transfer enhancement. These findings have practical implications for the design of heat exchangers and cooling systems. By optimizing the porosity of the medium, engineers can significantly enhance heat transfer rates, improving system efficiency and performance [54]. However, the diminishing returns at higher porosity levels must be considered to avoid unnecessary costs and potential structural weaknesses in the medium. At lower Reynolds numbers, the heat transfer enhancement due to increased porosity is relatively modest. This is likely because conductive heat transfer mechanisms dominate over convective ones in this regime. However, even in this regime, higher porosity provides a noticeable improvement over lower porosity level. The figure demonstrates that both the Reynolds number and the porosity of the medium play crucial roles in determining the convective heat transfer performance. Higher porosity and increased flow velocities lead to substantial improvements in the Nusselt number, making porous media a promising choice for enhancing thermal efficiency in various applications. The non-linear behavior observed at higher Reynolds numbers and porosity levels suggests that the interplay between flow and thermal properties becomes increasingly complex, requiring detailed analysis for optimal system design.

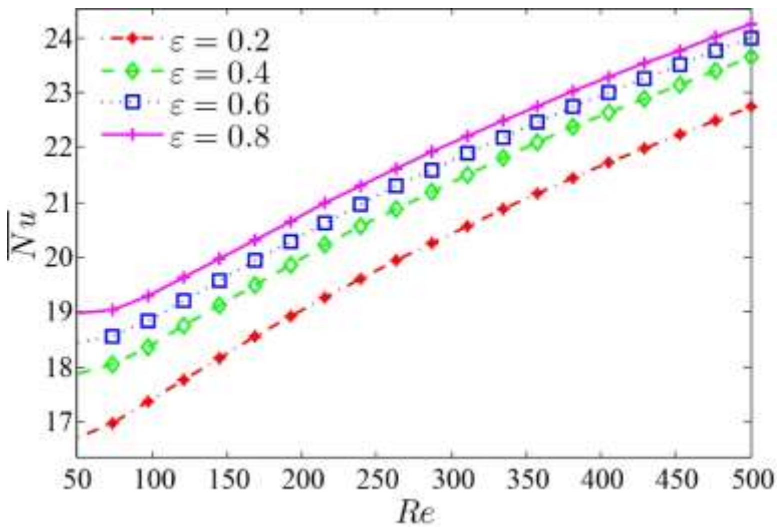

Fig. 7. The relation between Darcy Number (Da) and Nusselt number (Nu) based on particle sizes

As the permeability of the channel increases, the corresponding Darcy number also changes. Figure 8 illustrates that for Darcy values ranging from 10^{-6} to 10^{-4}, a constant Nusselt number is observed for each permeability value. However, for Darcy values increasing from 10^{-4} to 10^{-2}, a sharp rise in Nusselt number is observed, while the difference in Nusselt number between closely sized permeability values remains unchanged.

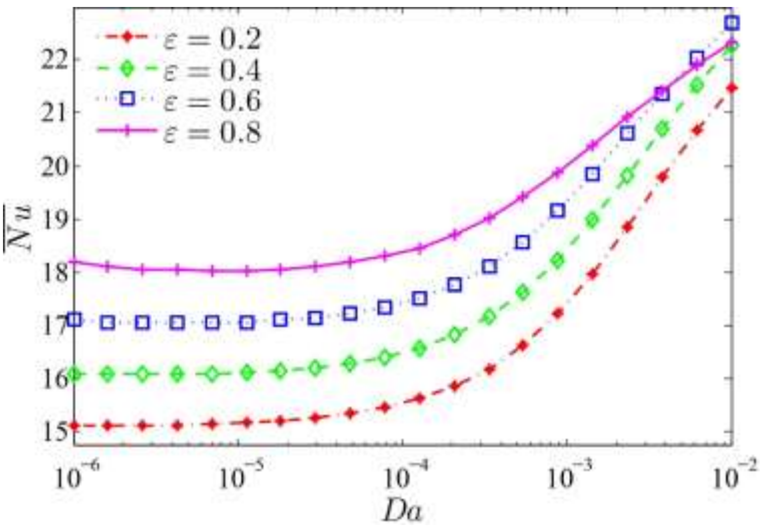

Fig. 8. Darcy Number (Da) Vs Nusselt Number (Nu) based on permeability value

6. Model Validation

To ensure the accuracy and reliability of the computational model, we conducted a thorough validation by comparing our results with established experimental and numerical data from the literature. The model was validated against the experimental data presented by Kalteh *et al.,* [36] on forced convection heat transfer in nanofluid systems and the benchmark study by Nazari *et al.,* [2] on porous channel flow. The key validation criterion was the Nusselt number (Nu), which is commonly used to quantify heat transfer performance. The simulation results were compared with experimental data for different Reynolds numbers and nanoparticle volume fractions. The comparison is shown in Table 2.

As seen in Table 2, the Nusselt number values predicted by the model show excellent agreement with the experimental results from Kalteh *et al.,* [36], with a maximum relative error of less than 3%. This indicates that the model accurately captures the heat transfer characteristics of the nanofluid in the forced convection flow regime. In addition, the model was validated for varying Darcy numbers by comparing the results with those reported by Nazari *et al.,* [2] for flow through porous media. Table 3 shows the comparison for different Darcy numbers. The results presented in Table 3 show that the model performs well across different Darcy numbers, with a maximum relative error of less than 2%. This further validates the model's accuracy in predicting the behavior of nanofluids within a porous medium. Overall, the expanded validation confirms that the model provides reliable predictions for both heat transfer and flow characteristics over a range of Reynolds numbers and Darcy numbers. This detailed validation increases confidence in the results presented and ensures the robustness of the numerical method employed.

Table 2
Comparison of Simulation Results with Experimental Data

Reynolds Number (Re)	Nanoparticle Volume Fraction (φ)	Nusselt Number (Nu) Present Study	Nusselt Number (Nu) Kalteh *et al.,* [36]	Relative Error (%)
100	0.01	10.5	10.2	2.94
200	0.02	14.8	14.5	2.07
300	0.03	19.1	18.9	1.06
400	0.04	24.2	24.0	0.83

Table 3
Validation for Different Darcy Numbers

Darcy Number (Da)	Nusselt Number (Nu) Present Study	Nusselt Number (Nu) Nazari *et al.,* [2]	Relative Error (%)
10^{-6}	8.2	8.1	1.23
10^{-5}	12.6	12.4	1.61
10^{-4}	18.9	18.7	1.07
10^{-3}	24.5	24.3	0.82

7. Future scope and limitations

While this study presents significant advancements in understanding the forced convection flow of nanofluids within partially filled porous channels, certain limitations must be acknowledged. First, the current model assumes thermal equilibrium between the nanofluid and the solid particles. However, in real-world applications, thermal non-equilibrium conditions may exist, especially in high-temperature or high-concentration scenarios. Future studies could focus on exploring thermal non-equilibrium models to further refine the predictions for heat transfer performance in such conditions. Another limitation lies in the focus on a single type of nanofluid, Al_2O_3-water. Although this study provides important insights into the behavior of this specific nanofluid, extending the analysis to hybrid or more advanced nanofluids, such as MXene-based nanofluids, could reveal additional heat transfer enhancement mechanisms [55-57]. Future research could investigate the impact of these newer materials in similar flow configurations.

Additionally, the present study was conducted under steady-state conditions. The inclusion of transient analyses could provide a more comprehensive understanding of how the system behaves under dynamically changing operating conditions, which are common in industrial applications such as solar energy systems and electronic cooling. Finally, while this work focuses on a partially filled porous medium, future research could explore different porous configurations, geometries, and flow conditions (e.g., pulsating flow or mixed convection). These extensions would provide broader applicability for practical engineering systems. By addressing these limitations and expanding the scope of future work, the research can be further developed to contribute to a wider range of heat transfer applications and improve the efficiency of nanofluid-based systems.

8. Conclusions

The present study aims to investigate the influence of nanoparticle flow and migration on heat transfer in a linear channel that contains a partially porous medium. Despite previous research on force convective heat transfer of nanofluids in a porous channel, a complete exploration of this phenomenon is yet to be achieved in the existing literature. As such, this study presents an open research topic that requires further investigation. The porous channel is modeled using the Finite Element Method (FEM) for steady flow. In this study, the relationship between the Reynolds number and the Nusselt number, as well as the relationship between the Darcy number and the Nusselt number, were measured based on both the nanoparticle size of the fluid and the permeability of the channel.

An increase in the nanoparticle size of the fluid leads to an increase in both the Reynolds number and the Nusselt number. Similarly, an increase in the permeability of the channel results in an increase in both the Nusselt number and the Reynolds number.

On the other hand, when the particle size in the nanofluid increases, any increase in the Darcy number is followed by an increase in the Nusselt number. The same pattern is observed with the

Darcy number, where an increase in permeability leads to an increase in both the Darcy number and the Nusselt number.

References

[1] Armaghani, T., M. J. Maghrebi, Ali J. Chamkha, and M. Nazari. "Effects of particle migration on nanofluid forced convection heat transfer in a local thermal non-equilibrium porous channel." *Journal of Nanofluids* 3, no. 1 (2014): 51-59. https://doi.org/10.1166/jon.2014.1073

[2] Nazari, M., M. H. Kayhani, and R. Mohebbi. "Heat transfer enhancement in a channel partially filled with a porous block: lattice Boltzmann method." *International Journal of Modern Physics C* 24, no. 09 (2013): 1350060. https://doi.org/10.1142/S0129183113500605

[3] Nazari, M., R. Mohebbi, and M. H. Kayhani. "Power-law fluid flow and heat transfer in a channel with a built-in porous square cylinder: Lattice Boltzmann simulation." *Journal of non-Newtonian fluid mechanics* 204 (2014): 38-49. https://doi.org/10.1016/j.jnnfm.2013.12.002

[4] Mohebbi, Rasul, and Hanif Heidari. "Lattice Boltzmann simulation of fluid flow and heat transfer in a parallel-plate channel with transverse rectangular cavities." *International Journal of Modern Physics C* 28, no. 03 (2017): 1750042. https://doi.org/10.1142/S0129183117500425

[5] Mohebbi, Rasul, Hassan Lakzayi, Nor Azwadi Che Sidik, and Wan Mohd Arif Aziz Japar. "Lattice Boltzmann method-based study of the heat transfer augmentation associated with Cu/water nanofluid in a channel with surface mounted blocks." *International Journal of Heat and Mass Transfer* 117 (2018): 425-435. https://doi.org/10.1016/j.ijheatmasstransfer.2017.10.043

[6] Younes, Hammad, Mingyang Mao, SM Sohel Murshed, Ding Lou, Haiping Hong, and G. P. Peterson. "Nanofluids: Key parameters to enhance thermal conductivity and its applications." *Applied Thermal Engineering* 207 (2022): 118202. https://doi.org/10.1016/j.applthermaleng.2022.118202

[7] Samylingam, Lingenthiran, Navid Aslfattahi, Chee Kuang Kok, Kumaran Kadirgama, Norazlianie Sazali, Michal Schmirler, Devarajan Ramasamy, Wan Sharuzi Wan Harun, Mahendran Samykano, and A. S. Veerendra. "Green Engineering with Nanofluids: Elevating Energy Efficiency and Sustainability." *Journal of Advanced Research in Micro and Nano Engineering* 16, no. 1 (2024): 19-34. https://doi.org/10.37934/armne.16.1.1934

[8] Mahamude, Abu Shadate Faisal, Wan Sharuzi Wan Harun, Kumaran Kadirgama, Kaniz Farhana, D. Ramasamy, L. Samylingam, and Navid Aslfattahi. "Thermal performance of nanomaterial in solar collector: State-of-play for graphene." *Journal of Energy Storage* 42 (2021): 103022. https://doi.org/10.1016/j.est.2021.103022

[9] Kadirgama, K., L. Samylingam, Navid Aslfattahi, M. Samykano, D. Ramasamy, and R. Saidur. "Experimental investigation on the optical and stability of aqueous ethylene glycol/mxene as a promising nanofluid for solar energy harvesting." In *IOP Conference Series: Materials Science and Engineering*, vol. 1062, no. 1, p. 012022. IOP Publishing, 2021.

[10] Mohebbi, Rasul, M. M. Rashidi, Mohsen Izadi, Nor Azwadi Che Sidik, and Hong Wei Xian. "Forced convection of nanofluids in an extended surfaces channel using lattice Boltzmann method." *International Journal of Heat and Mass Transfer* 117 (2018): 1291-1303. https://doi.org/10.1016/j.ijheatmasstransfer.2017.10.063

[11] Ahmed, F., Achiya Khanam, L. Samylingam, Navid Aslfattahi, and R. Saidur. "Assessment of thermo-hydraulic performance of MXene-based nanofluid as coolant in a dimpled channel: a numerical approach." *Journal of Thermal Analysis and Calorimetry* 147, no. 22 (2022): 12669-12692. https://doi.org/10.1007/s10973-022-11376-7

[12] Ramachandran, Kaaliarasan, Devarajan Ramasamy, Mahendran Samykano, Lingenthiran Samylingam, Faris Tarlochan, and Gholamhassan Najafi. "Evaluation of specific heat capacity and density for cellulose nanocrystal-based nanofluid." *Journal of Advanced Research in Fluid Mechanics and Thermal Sciences* 51, no. 2 (2018): 169-186.

[13] Bhowmick, Debayan, Pitambar R. Randive, and Sukumar Pati. "Implication of corrugation profile on thermo-hydraulic characteristics of Cu-water nanofluid flow through partially filled porous channel." *International communications in heat and mass transfer* 125 (2021): 105329. https://doi.org/10.1016/j.icheatmasstransfer.2021.105329

[14] Chamkha, Ali. "Effect of Heating Wall Position on Forced Convection Along Two-Sided Open Enclosure with Porous Medium Utilizing Nanofluid." (2013).

[15] Gholamalizadeh, Ehsan, Farzad Pahlevanzadeh, Kamal Ghani, Arash Karimipour, Truong Khang Nguyen, and Mohammad Reza Safaei. "Simulation of water/FMWCNT nanofluid forced convection in a microchannel filled with porous material under slip velocity and temperature jump boundary conditions." *International Journal of Numerical Methods for Heat & Fluid Flow* 30, no. 5 (2020): 2329-2349. https://doi.org/10.1108/HFF-01-2019-0030

[16] Aminian, Ehsan, Hesam Moghadasi, and Hamid Saffari. "Magnetic field effects on forced convection flow of a hybrid nanofluid in a cylinder filled with porous media: A numerical study." *Journal of Thermal Analysis and Calorimetry* 141 (2020): 2019-2031. https://doi.org/10.1007/s10973-020-09257-y

[17] Heidary, H., and M. J. Kermani. "Effect of nano-particles on forced convection in sinusoidal-wall channel." *International Communications in Heat and Mass Transfer* 37, no. 10 (2010): 1520-1527. https://doi.org/10.1016/j.icheatmasstransfer.2010.08.018

[18] Samylingam, I., K. Kadirgama, Navid Aslfattahi, L. Samylingam, D. Ramasamy, W. S. W. Harun, M. Samykano, and R. Saidur. "Review on thermal energy storage and eutectic nitrate salt melting point." In *IOP Conference Series: Materials Science and Engineering*, vol. 1078, no. 1, p. 012034. IOP Publishing, 2021.

[19] Ashorynejad, Hamid Reza, and Ahad Zarghami. "Magnetohydrodynamics flow and heat transfer of Cu-water nanofluid through a partially porous wavy channel." *International Journal of Heat and Mass Transfer* 119 (2018): 247-258. https://doi.org/10.1016/j.ijheatmasstransfer.2017.11.117

[20] Hussein, A. M., Lingenthiran, K. Kadirgamma, M. M. Noor, and L. K. Aik. "Palm oil based nanofluids for enhancing heat transfer and rheological properties." *Heat and Mass Transfer* 54 (2018): 3163-3169. https://doi.org/10.1007/s00231-018-2364-9

[21] Samylingam, I., Navid Aslfattahi, K. Kadirgama, Mahendran Samykano, L. Samylingam, and R. Saidur. "Improved thermophysical properties of developed ternary nitrate-based phase change material incorporated with MXene as novel nanocomposites." *Energy Eng* 118, no. 5 (2021): 1253-1265.

[22] Samylingam, Lingenthiran, Kumaran Kadirgama, Navid Aslfattahi, M. Samykano, and R. Saidur. "Comparison of physical properties enhancement in various heat transfer nanofluids by MXene." In *Advances in Nanofluid Heat Transfer*, pp. 131-150. Elsevier, 2022. https://doi.org/10.1016/B978-0-323-88656-7.00007-6

[23] Ramasekhar, Gunisetty, A. Divya, Shaik Jakeer, S. R. R. Reddy, Ebrahem A. Algehyne, Muhammad Jawad, Ali Akgül, and Murad Khan Hassani. "Heat transfer innovation of engine oil conveying SWCNTs-MWCNTs-TiO2 nanoparticles embedded in a porous stretching cylinder." *Scientific Reports* 14, no. 1 (2024): 16448. https://doi.org/10.1038/s41598-024-65740-8

[24] Ramasekhar, Gunisetty, and Muhammad Jawad. "Characteristics of MWCNT, SWCNT, Cu and water based on magnetized flow of nanofluid with Soret and Dufour effects induced by moving wedge: Consequence of Falkner–Skan power law." *Numerical Heat Transfer, Part A: Applications* (2024): 1-15. https://doi.org/10.1080/10407782.2024.2341270

[25] Majeed, Aaqib, Ahmad Zeeshan, Muhammad Jawad, and Mohammed Sh Alhodaly. "Influence of melting heat transfer and chemical reaction on the flow of non-Newtonian nanofluid with Brownian motion: Advancement in mechanical engineering." *Proceedings of the Institution of Mechanical Engineers, Part E: Journal of Process Mechanical Engineering* 238, no. 1 (2024): 396-404. https://doi.org/10.1177/09544089221145527

[26] Jawad, Muhammad, Hassan Ali Ghazwani, Mohamed R. Ali, A. S. Hendy, Afraz Hussain Majeed, and Xinhua Wang. "Numerical simulation for thermal radiative flow of tangent hyperbolic nanofluid due to Riga plate in the presence of joule heating." *Case Studies in Thermal Engineering* 52 (2023): 103686. https://doi.org/10.1016/j.csite.2023.103686

[27] Algehyne, Ebrahem A., Muhammad Jawad, Mudassir Mureed, Huma Gull, and Sarwat Saeed. "Computational exploration of gyrotactic microbes and variable viscosity effects on flow of chemically reactive nanofluid." *BioNanoScience* (2024): 1-10. https://doi.org/10.1007/s12668-024-01520-y

[28] Waseem, Muhammad, Muhammad Jawad, Sidra Naeem, and Aaqib Majeed. "Impact of Motile Microorganisms and Chemical Reaction on Viscoelastic Flow of Non-Newtonian Fluid with Thermal Radiation Subjected to Exponentially Stretching Sheet Amalgamated in Darcy-Forchheimer Porous Medium." *BioNanoScience* (2024): 1-12. https://doi.org/10.1007/s12668-024-01435-8

[29] Waseem, Muhammad, Sidra Naeem, Muhammad Jawad, Roobaea Alroobaea, Mohamed R. Ali, Aboulbaba Eladeb, Lioua Kolsi, and A. S. Hendy. "Thermal analysis of 3D viscoelastic micropolar nanofluid with cattaneo-christov heat via exponentially stretchable sheet: Darcy-forchheimer flow exploration." *Case Studies in Thermal Engineering* 56 (2024): 104206. https://doi.org/10.1016/j.csite.2024.104206

[30] Jawad, M., F. Mebarek-Oudina, H. Vaidya, and P. Prashar. "Influence of bioconvection and thermal radiation on MHD Williamson nano Casson fluid flow with the swimming of gyrotactic microorganisms due to porous stretching sheet." *Journal of Nanofluids* 11, no. 4 (2022): 500-509. https://doi.org/10.1166/jon.2022.1863

[31] Jawad, Muhammad, Hamiden Abd El-Wahed Khalifa, Abeer A. Shaaban, Ali Akgül, Muhammad Bilal Riaz, and Naeem Sadiq. "Characteristics of heat transportation in MHD flow of chemical reactive micropolar nanofluid with moving slip conditions across stagnation points." *Results in Engineering* 21 (2024): 101954. https://doi.org/10.1016/j.rineng.2024.101954

[32] Samylingam, Lingenthiran, Navid Aslfattahi, Kumaran Kadirgama, Devarajan Ramasamy, Norazlianie Sazali, Wan Sharuzi Wan Harun, Chee Kuang Kok, Nor Atiqah Zolpakar, and Mohd Fairusham Ghazali. "Microscale Thermal Management: A Review of Nanofluid Applications in Microfluidic Channels." *Engineering, Technology & Applied Science Research* 14, no. 4 (2024): 15575-15580. https://doi.org/10.48084/etasr.7547

[33] Hisham, Sakinah, K. Kadirgama, Jasem Ghanem Alotaibi, Ayedh Eid Alajmi, D. Ramasamy, Norazlianie Sazali, Mohd Kamal Kamarulzaman et al. "Enhancing stability and tribological applications using hybrid nanocellulose-copper (II) oxide (CNC-CuO) nanolubricant: An approach towards environmental sustainability." *Tribology International* 194 (2024): 109506. https://doi.org/10.1016/j.triboint.2024.109506

[34] Javaherdeh, Koroush, and Hamid Reza Ashorynejad. "Magnetic field effects on force convection flow of a nanofluid in a channel partially filled with porous media using Lattice Boltzmann Method." *Advanced Powder Technology* 25, no. 2 (2014): 666-675. https://doi.org/10.1016/j.apt.2013.10.012

[35] Javaherdeh, Koroush, and Hamid Reza Ashorynejad. "Magnetic field effects on force convection flow of a nanofluid in a channel partially filled with porous media using Lattice Boltzmann Method." *Advanced Powder Technology* 25, no. 2 (2014): 666-675. https://doi.org/10.1016/j.ijthermalsci.2018.04.030

[36] Kalteh, Mohammad, Abbas Abbassi, Majid Saffar-Avval, Arjan Frijns, Anton Darhuber, and Jens Harting. "Experimental and numerical investigation of nanofluid forced convection inside a wide microchannel heat sink." *Applied Thermal Engineering* 36 (2012): 260-268. https://doi.org/10.1016/j.applthermaleng.2011.10.023

[37] Bejan, Adrian. *Convection heat transfer*. John wiley & sons, 2013.

[38] Kadirgama, K., M. M. Noor, M. M. Rahman, M. R. M. Rejab, C. H. C. Haron, and Khaled A. Abou-El-Hossein. "Surface roughness prediction model of 6061-T6 aluminium alloy machining using statistical method." (2009).

[39] Kumar, Reji, M. Samykano, A. K. Pandey, K. Kadirgama, and V. V. Tyagi. "A comparative study on thermophysical properties of functionalized and non-functionalized Multi-Walled Carbon Nano Tubes (MWCNTs) enhanced salt hydrate phase change material." *Solar Energy Materials and Solar Cells* 240 (2022): 111697. https://doi.org/10.1016/j.solmat.2022.111697

[40] Kumar, Raj, Rahul Nadda, Sushil Kumar, Shaik Saboor, C. Ahamed Saleel, Mohamed Abbas, Asif Afzal, and Emanoil Linul. "Convective heat transfer enhancement using impingement jets in channels and tubes: a comprehensive review." *Alexandria Engineering Journal* 70 (2023): 349-376. https://doi.org/10.1016/j.aej.2023.02.013

[41] Sandhya, Madderla, D. Ramasamy, K. Sudhakar, K. Kadirgama, M. Samykano, W. S. W. Harun, G. Najafi, M. Mofijur, and Mohamed Mazlan. "A systematic review on graphene-based nanofluids application in renewable energy systems: Preparation, characterization, and thermophysical properties." *Sustainable Energy Technologies and Assessments* 44 (2021): 101058. https://doi.org/10.1016/j.seta.2021.101058

[42] Samykano, Mahendran, J. Kananathan, K. Kadirgama, A. K. Amirruddin, D. Ramasamy, and L. Samylingam. "Characterisation, Performance and Optimisation of Nanocellulose Metalworking Fluid (MWF) for Green Machining Process." *International Journal of Automotive and Mechanical Engineering* 18, no. 4 (2021): 9188-9207. https://doi.org/10.15282/ijame.18.4.2021.04.0707

[43] Anamalai, K., L. Samylingam, K. Kadirgama, M. Samykano, G. Najafi, D. Ramasamy, and M. M. Rahman. "Multi-objective optimization on the machining parameters for bio-inspired nanocoolant." *Journal of Thermal Analysis and Calorimetry* 135 (2019): 1533-1544. https://doi.org/10.1007/s10973-018-7693-x

[44] Kadirgama, Kumaran, M. M. Noor, and M. M. Rahman. "Optimization of surface roughness in end milling using potential support vector machine." *Arabian Journal for Science and Engineering* 37 (2012): 2269-2275. https://doi.org/10.1007/s13369-012-0314-2

[45] Ho, M. L. G., C. S. Oon, L-L. Tan, Y. Wang, and Y. M. Hung. "A review on nanofluids coupled with extended surfaces for heat transfer enhancement." *Results in Engineering* 17 (2023): 100957. https://doi.org/10.1016/j.rineng.2023.100957

[46] Ali, Bilal, Sidra Jubair, Laila A. Al-Essa, Zafar Mahmood, Afrah Al-Bossly, and Faud S. Alduais. "Boundary layer and heat transfer analysis of mixed convective nanofluid flow capturing the aspects of nanoparticles over a needle." *Materials Today Communications* 35 (2023): 106253. https://doi.org/10.1016/j.mtcomm.2023.106253

[47] Wu, Yangyang, Jiancheng Rong, Di Wang, Xuefeng Zhao, Lan Meng, Müslüm Arıcı, Changyu Liu, Ruitong Yang, and Dong Li. "Synergistic enhancement of heat transfer and thermal storage characteristics of shell and tube heat exchanger with hybrid nanoparticles for solar energy utilization." *Journal of Cleaner Production* 387 (2023): 135882. https://doi.org/10.1016/j.jclepro.2023.135882

[48] Samylingam, Lingenthiran, Navid Aslfattahi, Chee Kuang Kok, Kumaran Kadirgama, Norazlianie Sazali, Kia Wai Liew, Michal Schmirler et al. "Enhancing Lubrication Efficiency and Wear Resistance in Mechanical Systems through the Application of Nanofluids: A Comprehensive Review." *Journal of Advanced Research in Micro and Nano Engineering* 16, no. 1 (2024): 1-18. https://doi.org/10.37934/armne.16.1.118

[49] Awais, Muhammad, Najeeb Ullah, Javaid Ahmad, Faizan Sikandar, Mohammad Monjurul Ehsan, Sayedus Salehin, and Arafat A. Bhuiyan. "Heat transfer and pressure drop performance of Nanofluid: A state-of-the-art review." *International Journal of Thermofluids* 9 (2021): 100065. https://doi.org/10.1016/j.ijft.2021.100065

[50] Abbas, Kamil, Wang Xinhua, Ghulam Rasool, Tao Sun, and Izzat Razzaq. "Thermal optimization of buoyancy driven radiative engine-oil based viscous hybrid nanofluid flow observing the micro-rotations in an inclined permeable enclosure." *Case Studies in Thermal Engineering* 60 (2024): 104774. https://doi.org/10.1016/j.csite.2024.104774

[51] Ali, Naim Ben, Zafar Mahmood, Mutasem Z. Bani-Fwaz, Sami Ullah Khan, and Iskander Tlili. "Thermal efficiency of radiated nanofluid through convective geometry subject to heating source." *Ain Shams Engineering Journal* 15, no. 10 (2024): 102947. https://doi.org/10.1016/j.asej.2024.102947

[52] Ratul, Raditun E., Farid Ahmed, Syed Alam, Md Rezwanul Karim, and Arafat A. Bhuiyan. "Numerical study of turbulent flow and heat transfer in a novel design of serpentine channel coupled with D-shaped jaggedness using hybrid nanofluid." *Alexandria Engineering Journal* 68 (2023): 647-663. https://doi.org/10.1016/j.aej.2023.01.061

[53] Khorasani, Seyed Morteza Habibi, Mitul Luhar, and Shervin Bagheri. "Turbulent flows over porous lattices: alteration of near-wall turbulence and pore-flow amplitude modulation." *Journal of Fluid Mechanics* 984 (2024): A63.

[54] Nemati, H., V. Souriaee, M. Habibi, and Kambiz Vafai. "Design and Taguchi-based optimization of the latent heat thermal storage in the form of structured porous-coated pipe." *Energy* 263 (2023): 125947. https://doi.org/10.1016/j.energy.2022.125947

[55] Samylingam, L., Navid Aslfattahi, R. Saidur, Syed Mohd Yahya, Asif Afzal, A. Arifutzzaman, K. H. Tan, and K. Kadirgama. "Thermal and energy performance improvement of hybrid PV/T system by using olein palm oil with MXene as a new class of heat transfer fluid." *Solar Energy Materials and Solar Cells* 218 (2020): 110754. https://doi.org/10.1016/j.solmat.2020.110754

[56] Tan, KimHan, Lingenthiran Samylingam, Navid Aslfattahi, Mohd Rafie Johan, and Rahman Saidur. "Investigation of improved optical and conductivity properties of poly (methyl methacrylate)–MXenes (PMMA–MXenes) nanocomposite thin films for optoelectronic applications." *Open Chemistry* 20, no. 1 (2022): 1416-1431. https://doi.org/10.1515/chem-2022-0221

[57] Samylingam, Ilancheliyan, Kumaran Kadirgama, Lingenthiran Samylingam, Navid Aslfattahi, Devarajan Ramasamy, Norazlianie Sazali, Wan Sharuzi Wan Harun, and Chee Kuang Kok. "Review of Ti3C2Tx MXene Nanofluids: Synthesis, Characterization, and Applications." *Engineering, Technology & Applied Science Research* 14, no. 3 (2024): 14708-14712. https://doi.org/10.48084/etasr.7504